

Scanning-free BOTDA based on ultra-fine digital optical frequency comb

Chao Jin,¹ Nan Guo,¹ Yuanhua Feng,² Liang Wang,¹ Hao Liang,² Jianping Li,² Zhaohui Li,^{2,*} Changyuan Yu^{3,4} and Chao Lu¹

¹Photonics Research Centre, The Hong Kong Polytechnic University, Hong Kong, China

²Institute of Photonics Technology, Jinan University, Guangzhou 510632, China

³Department of Electrical and Computer Engineering, National University of Singapore, 117576, Singapore

⁴A*STAR Institute for Infocomm Research (IIR), 138632, Singapore

*li_zhaohui@hotmail.com

Abstract: We realize a scanning-free Brillouin optical time domain analyzer (BOTDA) based on an ultra-fine digital optical frequency comb (DOFC) with 1.95MHz frequency spacing and 2GHz bandwidth. The DOFC can be used to reconstruct the Brillouin gain spectrum (BGS) and locate the Brillouin frequency shift (BFS) without frequency scanning and thus can improve the measurement speed about 100 times compared with the conventional BOTDA. This scanning-free BOTDA scheme has also been demonstrated experimentally with 51.2m spatial resolution over 10km standard single mode fiber (SSMF) and with resolution of 1.5°C for temperature and 43.3με for strain measurement respectively.

©2015 Optical Society of America

OCIS codes: (060.2310) Fiber optics; (060.2370) Fiber optics sensors; (290.5900) Scattering, stimulated Brillouin.

References and links

1. X. Bao and L. Chen, "Recent progress in optical fiber sensors based on Brillouin scattering at university of Ottawa," *Photon. Sensors* **1**(2), 102–117 (2011).
 2. L. Thevenaz, M. Nikles, A. Fellay, M. Facchini, and P. A. Robert, "Truly distributed strain and temperature sensing using embedded optical fibers," *Proc. SPIE* **3330**, 301–314 (1998).
 3. X. Bao, M. DeMerchant, A. Brown, and T. Bremner, "Tensile and compressive strain measurement in the lab and field with the distributed Brillouin scattering sensor," *J. Lightwave Technol.* **19**(11), 1698–1704 (2001).
 4. R. Bernini, A. Minardo, and L. Zeni, "Dynamic strain measurement in optical fibers by stimulated Brillouin scattering," *Opt. Lett.* **34**(17), 2613–2615 (2009).
 5. Y. Peled, A. Motil, L. Yaron, and M. Tur, "Slope-assisted fast distributed sensing in optical fibers with arbitrary Brillouin profile," *Opt. Express* **19**(21), 19845–19854 (2011).
 6. Y. Peled, A. Motil, I. Kressel, and M. Tur, "Monitoring the propagation of mechanical waves using an optical fiber distributed and dynamic strain sensor based on BOTDA," *Opt. Express* **21**(9), 10697–10705 (2013).
 7. Y. Peled, A. Motil, and M. Tur, "Fast Brillouin optical time domain analysis for dynamic sensing," *Opt. Express* **20**(8), 8584–8591 (2012).
 8. X. Bao, C. Zhang, W. Li, M. Eisa, S. El-Gamal, and B. Benmokrane, "Monitoring the distributed impact wave on a concrete slab due to the traffic based on polarization dependence on stimulated Brillouin scattering," *Smart Mater. Struct.* **17**(1), 015003 (2008).
 9. A. Voskoboinik, W. Jian, B. Shamee, S. R. Nuccio, L. Zhang, M. Chitgarha, A. E. Willner, and M. Tur, "SBS-Based Fiber Optical Sensing Using Frequency-Domain Simultaneous Tone Interrogation," *J. Lightwave Technol.* **29**(11), 1729–1735 (2011).
 10. A. Voskoboinik, O. F. Yilmaz, A. W. Willner, and M. Tur, "Sweep-free distributed Brillouin time-domain analyzer (SF-BOTDA)," *Opt. Express* **19**(26), B842–B847 (2011).
 11. A. Voskoboinik, D. Rogawski, H. Huang, Y. Peled, A. E. Willner, and M. Tur, "Frequency-domain analysis of dynamically applied strain using sweep-free Brillouin time-domain analyzer and sloped-assisted FBG sensing," *Opt. Express* **20**(26), B581–B586 (2012).
 12. X. Yi, Z. Li, Y. Bao, and K. Qiu, "Characterization of Passive Optical Components by DSP-Based Optical Channel Estimation," *IEEE Photon. Technol. Lett.* **24**(6), 443–445 (2012).
 13. C. Jin, Y. Bao, Z. Li, T. Gui, H. Shang, X. Feng, J. Li, X. Yi, C. Yu, G. Li, and C. Lu, "High-resolution optical spectrum characterization using optical channel estimation and spectrum stitching technique," *Opt. Lett.* **38**(13), 2314–2316 (2013).
 14. M. A. Soto and L. Thévenaz, "Modeling and evaluating the performance of Brillouin distributed optical fiber sensors," *Opt. Express* **21**(25), 31347–31366 (2013).
-

1. Introduction

In recent decades, the increasing demands for structural health monitoring have driven the research and development of sensor systems capable of distributed monitoring of temperature and strain change along the fiber [1]. Among them, Brillouin optical time domain analyzer (BOTDA) has shown a promising prospect in many application scenarios. However, the acquisition time of BOTDA is normally in the order of few minutes, mainly owing to the need for scanning the probe frequency to obtain the Brillouin gain spectrum (BGS) in order to locate the Brillouin frequency shift (BFS) induced by temperature or strain along the fiber. This is time consuming and thus cannot meet the requirement in the case of fast distributed monitoring system [2, 3]. As a result, BOTDA systems can only be used in slow analysis and static measurement till now. On the other hand, the possibility to extend the distributed optical fiber sensors to dynamic measurements would be of special interest in many application fields, such as measurement of vibrations in civil or aeronautic structures which require a monitoring response in the range of seconds or even less. One of main methods to realize the real time BOTDA system is based on avoiding the scanning of the probe signal.

Recently, several adaptations are proposed to realize the frequency scanning-free BOTDA system. For example, slope-assisted BOTDA is realized based on tuning the frequency of probe optical signal to the half of BGS. In this way, BFS can be mapped as intensity variation of Stokes pulse [4–7]. However, the dynamic range of strain measurement using this scheme is limited by the linear range of the BGS. Another scheme is proposed using polarization dependence of the Brillouin gain [8]. Recently, another kind of scanning-free BOTDA is proposed based on multiple probe and pump pairs, the frequency difference of each probe-pump pairs lies in different position of BGS, so allowing for the fast measurement of strain/temperature change along the fiber [9–11]. A modification of this scheme can be realized based on only single pump signal but comprising multiple frequency tones [10]. The number of pump-probe pairs is finite due to the bandwidth of BGS and frequency spacing of pump and probe signals, and thus we cannot optimize the measurement range and resolution simultaneously for this scheme.

Optical frequency comb has already found important applications in precise metrology and many other applications [12, 13]. Recently, we propose a digitally generated optical frequency comb to realize ultra-fine and fast optical spectral analysis without frequency scanning and thus can be potentially used to realize a fast BOTDA. In this paper, we study the performance of a fast BOTDA based on the digital optical frequency comb (DOFC), which can locate the BFS without frequency scanning. The scanning-free BOTDA system is demonstrated experimentally with 51m spatial resolution over 10km standard single mode fiber. The resolution and range are 1.5°C and 30°C for temperature measurement respectively. The resolution and range are 43.3μ ϵ and 900μ ϵ for strain measurement respectively.

2. Sensing principle, generation and demodulation of DEFC

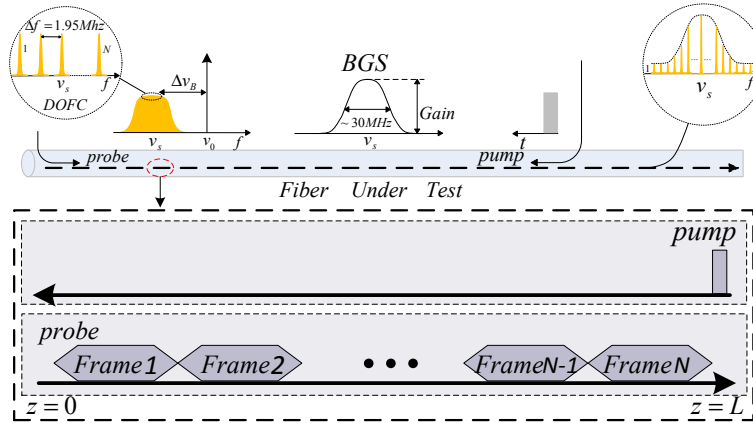


Fig. 1. Schematic representation of the principle of DOFC based BOTDA.

In the proposed frequency sweep-free BOTDA sensing scheme, DOFC is used as probe to detect BGS and locate BFS. The sensing principle is illustrated in Fig. 1. A wideband pulsed DOFC probe at 1550nm is launched into the fiber under test (FUT) at position $z = 0$, while a single tone pump is introduced from the opposite direction at position $z = L$. As shown in Fig. 1, the multi-tone optical probe signal distribute symmetrically around the typical BFS (~ 11 GHz) in single mode fiber in a frequency range of 1GHz, and it has a flat top within the Brillouin linewidth. In the FUT, the consecutive but separated frames interact with pump in sequence. And the spectrum of the DOFC probe is reshaped by frequency selective Brillouin amplification induced by stimulated Brillouin scattering (SBS) process. Therefore, the distributed BFS can be obtained by detecting the corresponding digital electrical frequency comb (DEFC) after photo detection, and the environmental properties along the fiber such as temperature and strain distribution can be obtained accordingly.

The generation and demodulation of DEFC is shown in Fig. 2. A proper pulse train of data with unit amplitude is transformed to DEFC by inverse fast Fourier transform (IFFT) and fed into an arbitrary waveform generator (AWG) operating at the sampling rate of 2G Samples/s. Each DEFC frame is separated by a Guard Interval (GI) to avoid inter-frame distortions. Then base band DEFC frames are up-converted by mixing with 11 GHz sinusoidal wave to cover the BFS range in the distributed sensor system. We must make clear that the duration length of DEFC frame T is inversely related to the resolution of frequency comb Δf —the finer frequency resolution, the longer duration length.

At the receiver end, the beating signal between optical carrier and the upper optical sideband generated by the same laser through electro-optic modulation is detected and converted to digital domain through an analog to digital converter (ADC). Processing methods including frame synchronization, frequency down-conversion and Fast Fourier transform (FFT) are used to demodulate the DEFC frames before analyzing amplification information carried on each frequency comb line, i.e. the BGS.

Unlike the conventional BOTDA system, the location principle of DOFC-BOTDA is based on consecutive but separated DEFC frames. Each frame, collected by oscilloscope chronologically, contains the information of peak gain frequency of a section of fiber it covered. In this way, the spatial resolution of the system is limited by the duration length of frame. For example, a DEFC frame with duration length of 50ns corresponds to a spatial resolution of 5 meters.

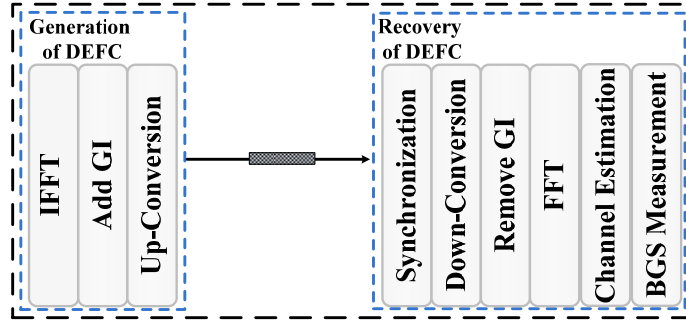


Fig. 2. Generation and demodulation of digital electrical frequency comb. IFFT: Inverse fast Fourier Transform; FFT: Fast Fourier Transform; GI: Guard Interval.

The power spectrum of the generated baseband DEFC is shown in Fig. 3, which are orthogonal multi-carrier signal. It is worth noting that the frequency range of DEFC is limited by sample rate of AWG. In our configuration, most of power is distributed within the range of 1GHz. The power spectrum within 1GHz is flat, and the power densities beyond this range drop dramatically, which is beneficial to the noise resistance capability. In our application, 1024 subcarriers each carried with unit amplitude signal is inversely transformed to time domain by IFFT, generating an orthogonal multi-carrier signal. The inset picture in Fig. 3 shows the zoomed view of generated DEFC with frequency spacing of 1.95MHz (2GHz/1024), corresponding to a temperature/strain resolution of 1.5°C/43.3 μ e respectively. Here, the frequency spacing of DEFC can be further reduced by increasing the length of IFFT.

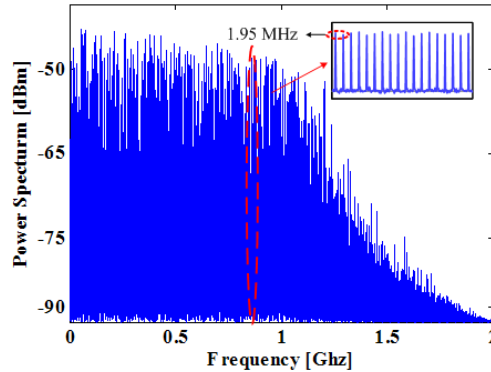


Fig. 3. Power spectrum of digital electrical frequency comb.

3. Experimental setup

The experimental setup of scanning-free BODTA based on DOFC is shown in Fig. 4. In this experiment, a tunable laser operating at 1550nm with 100 kHz linewidth is split into two parts to serve as pump and probe signal respectively by using a 50/50 optical coupler.

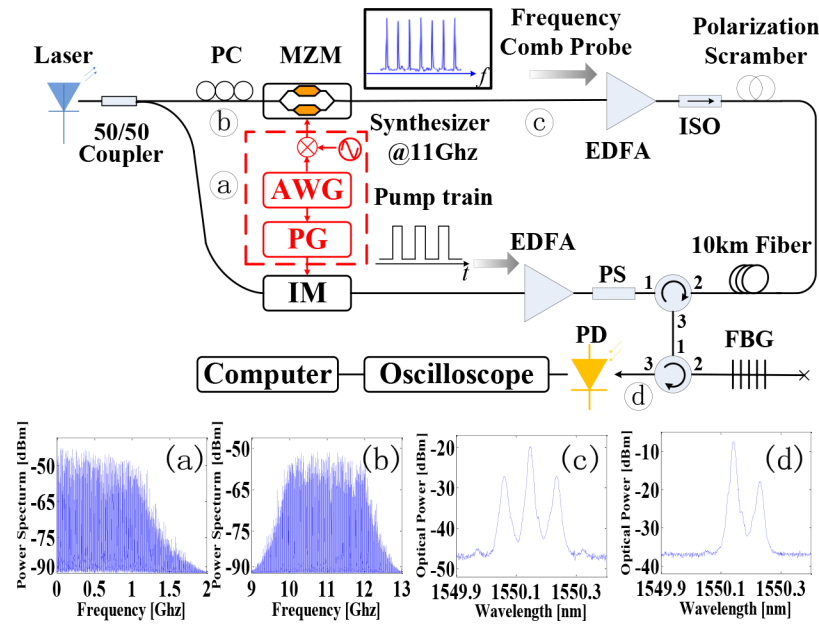


Fig. 4. Scanning-free BOTDA experiment Setup. AWG: arbitrary waveform generator; MZM: Mach-Zehnder modulator; EDFA: erbium-doped fiber amplifier; OSA: optical spectrum analyzer; ISO: isolator; PG: pulse generator; IM: intensity modulator; PC: polarization controller; PS: polarization scrambler; FBG: fiber Bragg grating; PD: photo detector.

At the probe signal side the baseband DEFC is first up-converted to 11GHz by mixing with an 11GHz radio frequency (RF) signal using a RF mixer in order to cover the whole BGS, as shown in the Fig. 4(b). We can find that the bandwidth of the DEFC become 2GHz from 1GHz after the frequency up-conversion. The duration length of each DEFC frame is 512ns, corresponding to a spatial resolution of 51.2m. The up-converted DEFC is then modulated onto laser through a Mach-Zehnder modulator (MZM) biased at quadrature point to generate double sideband DOFC, as shown in Fig. 4(c). The DOFC is amplified by Erbium doped fiber amplifier (EDFA) to 0dBm, and then pass the FUT for distributed Brillouin interaction with the pump signal. In this process, the environmental properties along the fiber, such as temperature and strain variation are recorded on the amplitude, phase and polarization of each frequency comb line of DOFC.

At the pump signal side, electrical pulse trains generated from the pulse generator is modulated onto the pump laser through a high extinction ratio optical intensity modulator biased at null-transmission point. In this way, the optical pulse of 100ns width and 8.2 kHz repetition rate is generated with extinction ratio about 35dB. The average pump signal power is ~0dBm. Besides, a replica of the same electrical pulse is used to trigger the real-time oscilloscope in order to facilitate data acquisition and averaging. The pump pulse is sent to EDFA for amplification before launched into FUT. A polarization scrambler is placed in front of the optical circulator to alleviate polarization dependent fluctuations for Brillouin effect between the pump and probe signals.

At the receiver, after Brillouin scattering frequency selective amplification, the probe signal from the FUT is first filtered by a narrow band fiber Bragg grating to block DOFC at the lower sideband before entering the photo detector with 12GHz bandwidth, as shown in Fig. 4(d). A ~11GHz electrical signal is obtained by beating between optical carrier and DOFC signal at upper sideband and digitized by a real-time oscilloscope working at 50 GS/s sampling rate. The collected DEFC signal is transferred to PC for digital frequency down-conversion and further digital signal processing to locate the information of BFS.

4. Experimental results

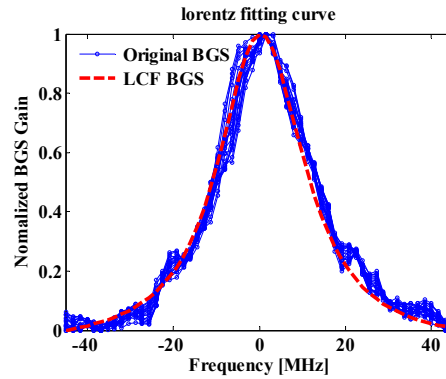


Fig. 5. Original measured BGS and Lorentz fitting curve.

The received beating signals are first averaged 100 times to improve the measurement accuracy as well as to obtain a desirable signal-to-noise ratio (SNR). The original BGS without any applied environment variance are illustrated as the blue curve in Fig. 5. The BGS after Lorentz fitting is shown as a red curve in Fig. 5, with the estimated full maximum (FWHM) to be ~ 30 MHz.

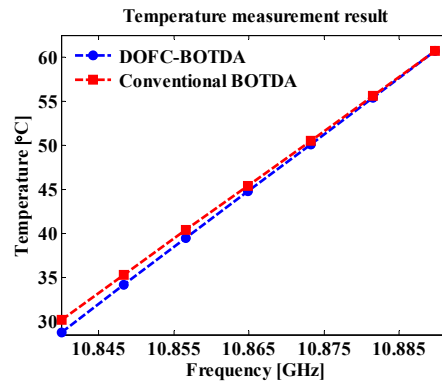


Fig. 6. Linear fitting of temperature measurement results using conventional BOTDA and DOFC-BOTDA.

In the temperature measurement configuration, we heat the first 51m fiber of 10km fiber by using thermal chamber. Temperature setup is adjusted from the 30°C to 60°C changing with 5°C step. The linear fitting result of measured BFS change with the temperature variation is depicted in Fig. 6. Temperature coefficient for this fiber is calculated to be $0.79^{\circ}\text{C}/\text{MHz}$, which is similar to the result of conventional BOTDA. Maximum temperature measurement deviation is about 0.5°C .

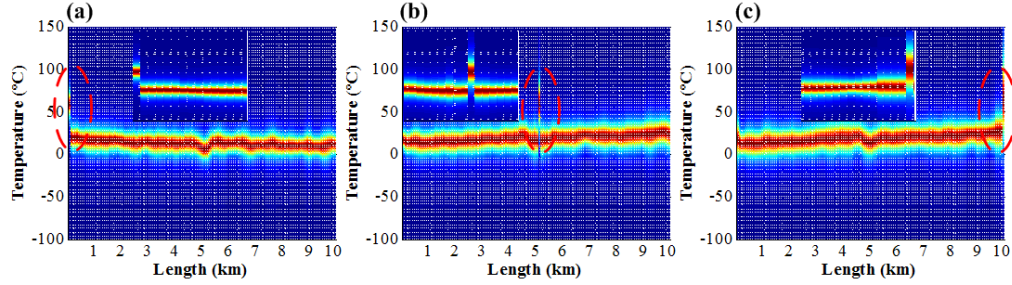


Fig. 7. Temperature measurement at different position: (a) first 51m fiber, (b) middle 51m fiber (c) last 51m fiber of 10km fiber under test.

In order to evaluate the performance of the proposed method for distributed sensing, measurements at three different positions along the 10km fiber are carried out: they are the first 51m fiber, middle 51m fiber and the last 51m fiber along the 10km fiber under test. We apply the same temperature of 60°C on aforementioned fiber section at different locations along the fiber. Figure 7 shows the obtained BFS as a function of position after averaging 100 times. The inset pictures in Fig. 7 provide the zoomed view of the measured temperature changes after fitting the measured spectrum with Lorentz curve.

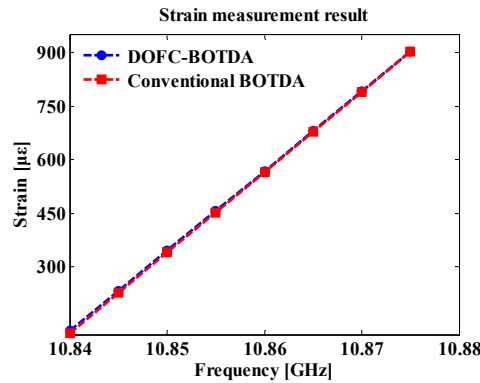


Fig. 8. Linear fitting of strain measurement results using conventional BOTDA and DOFC-BOTDA.

We also carried out a strain measurement based on almost the same experimental setup. One end of 51m fiber is first wound and fixed on base plate of the optical experiment bench, while the other end of this 51m fiber is stretched by displacement platform to gradually increase the strain applied on the fiber under test. The strain is adjusted from 0 $\mu\epsilon$ to 900 $\mu\epsilon$ with a step of about 110 $\mu\epsilon$ corresponding to frequency shift step of 5MHz. Figure 8 shows the linear fitting result of BFS as a function of strain at the first 51m fiber. Good linear relation is achieved within the strain measurement range. The measurement deviation is less than 19 $\mu\epsilon$, and BFS coefficient is about 22.5 $\mu\epsilon$ /MHz.

In our setup, the time needed for each acquisition is about 100 μs , and 100 acquisitions are needed in a single measurement to improve the obtained SNR, resulting a total measurement time of approximately 10ms. The obtained SNR at the end of FUT degrades slightly (~ 0.6 dbm) compared with conventional BOTDA due to the multiple power transfer occurred in the SBS process between single pump and DOFC. BOTDA sensors, however, typically operates in a small gain regime [14] (i.e. the relative power transfer is actually very low). This degradation is estimated to be minor compared with the Brillouin gain. As reported above, performance of conventional BOTDA and DOFC-BOTDA are compared. In the conventional BOTDA, the obtained SNR at the far end of fiber is 8.76dB. While in DOFC-BOTDA, this figure degraded slightly to 8.1dB.

5. Conclusions

In summary, a scanning-free BOTDA is presented and demonstrated experimentally. Based on DOFC, the BGS can be reconstructed without frequency-sweep thus greatly improves the measurement speed. Distributed temperature and strain measurements over 10km fiber range are conducted and compared with the conventional BOTDA. Favorable results are obtained and show a good agreement with conventional BOTDA.

Acknowledgments

The authors would like to acknowledge the support of National High Technology 863 Research and Development Program of China (No. 2013AA013300), (No. 2013AA013403), National Natural Science Foundation of China (NSFC) under Grant No. 61435006 and 61377093 and New Century Excellent Talents in University (NCET-12-0679) as well as Hong Kong RGC GRF grant (PolyU 5208/13E) .